

Lipase mediated enzymatic kinetic resolution of phenylethyl halohydrins acetates: A case of study and rationalization

Thiago de Sousa Fonseca^a, Kimberly Benedetti Vega^a, Marcos Reinaldo da Silva^a, Maria da Conceição Ferreira de Oliveira^a, Telma Leda Gomes de Lemos^a, Davila Zampieri^a, Martina Letizia Contente,^b Francesco Molinari,^b Marco Cespugli^c, Sara Fortuna^c, Lucia Gardossi^c, and Marcos Carlos de Mattos^{a*}

^a*Department of Organic and Inorganic Chemistry, Laboratory of Biotechnology and Organic Synthesis (LABS), Federal University of Ceará, Campus do Pici, Postal Box 6044, 60455-970 Fortaleza, Ceará, Brazil*

^b*Department of Food, Environmental and Nutritional Sciences (DEFENS), University of Milan, Via Mangiagalli 25, 20133 Milan, Italy*

^c*Laboratory of Applied and Computational Biocatalysis, Dipartimento di Scienze Chimiche e Farmaceutiche, Università degli Studi di Trieste, Via Licio Giorgieri 1, 34127, Trieste, Italy*

ABSTRACT

Racemic phenylethyl halohydrins acetates containing several groups attached to the aromatic ring were resolved via hydrolysis reaction in the presence of lipase B from *Candida antarctica* (Novozym[®] 435). In all cases the kinetic resolution was highly selective ($E > 200$) leading to the corresponding (*S*)- β -halohydrin with $ee > 99\%$. However, the time required for an ideal 50% conversion ranged from 15 min for 2,4-dichlorophenyl chlorohydrin acetate to 216 h for 2-chlorophenyl bromohydrin acetate. Six chlorohydrins and five bromohydrins were evaluated, the latter being less reactive. For the β -brominated substrates steric hindrance on the aromatic ring plays a crucial role, which is not observed for the β -chlorinated derivatives. To shed light on the different reaction rates docking studies of all the substrates have been carried out using molecular dynamics simulations. The computational data obtained for the β -brominated substrates based on the parameters analyzed such as NAC (near attack conformation), distance between Ser-O and carbonyl-C and oxyanion site stabilization are in agreement with the experimental results. On the other hand, the data obtained for β -chlorinated substrates suggest that physical aspects such as high hydrophobicity or induced change in the conformation of the enzymatic active site are more relevant aspects when compared to steric hindrance effects.

Introduction

Halohydrins are an important class of organic compounds used as intermediates in the synthesis of several bioactive substances with high added value [1-5]. One of the most usual protocols for the preparation of halohydrins is the ring-opening of epoxides in the presence of hydrogen halides or hydrohalogenic acids. However, some drawbacks associated with this process, such as the formation of by-products and the intolerance of acid-sensitive groups, have led to the development of new, more effective and environmentally friendly procedures [1-5]. Some of these methods include the ring-opening of epoxides with halides via phase transfer catalysis (PTC) in the presence of quaternized amino functionalized cross-linked polyacrylamide as an efficient heterogeneous catalyst [6]; use of ionic liquids as recyclable solvents for the regioselective ring-opening of epoxides with lithium halides under mild and neutral conditions [1]; regioselective ring opening of oxiranes with tetrabutylammonium halide in water in the presence of β -cyclodextrin [2]; use of bismuth(III) salts for the regioselective ring opening of epoxides [3]; halohydroxylation of olefin derivatives using chloramine T trihydrate, 1,3-dichloro-5,5-dimethylhydantoin (DCDMH) or *N*-bromoacetamide (AcNHBr) as the halogen source under mild conditions [4] and regioselective ring opening of epoxides using cross-linked poly(4-vinylpyridine) supported HCl and HBr under solvent-free conditions [5].

Besides these protocols, the methodologies for the preparation of chiral halohydrins are of relevant importance, which are versatile intermediates in the synthesis of useful drugs and pharmaceuticals, such as (*S*)- β -blockers propranolol, toliprol, moprolol, alprenolol, penbutenol, practolol, oxprenolol [7], sotalol [8] atenolol [7,9,10] and pindolol [11]. In addition, drugs such as (*R*)-fluoxetine [12-14], (*R*)-clorprenaline [8], (*R*)-duloxetine [14,15] and the antifungal agents, such as miconazole, econazole, sertaconazole [16] and luliconazole [17] were prepared starting from chiral halohydrins as intermediates. The most known process for obtaining chiral halohydrins is the ring-opening of chiral epoxides. However, this method has the disadvantage of the formation of regioisomers [18]. An effective approach to circumvent this problem is the asymmetric reduction of prochiral α -halo ketones by chiral catalysts such as oxazaborolidine with borane [19] or Ru [20]. It should be noted that chiral halohydrins were obtained by dynamic kinetic resolution (DKR) of α -halo indanones or tetralones using Ru-based Noyori/Ikariya catalysts [21].

Biocatalysis offers a green alternative tool over conventional chemical processes to obtaining chiral halohydrins. Bioprocesses include the reduction of the corresponding α -haloketones in the presence of microbial cells [22,23] or isolated enzymes (KREDs) [16,24,25] and lipase-catalyzed kinetic resolution of racemic halohydrins or their corresponding esters [7,10,11,15,17,26,27], being the latter the most used. The use of lipases is mainly due to the characteristics of the regio-, chemo- and enantioselectivity in the resolution process of racemates, without the use of cofactors. Moreover, this class of enzymes has generally excellent stability in the presence of organic solvents, facilitating the solubility of organic substrate to be modified [28,29]. It should be noted that lipases have been used to catalyze both kinetic resolution processes, the acetylation of halohydrins or the hydrolysis of the corresponding esters. Some examples include the use of *Pseudomonas fluorescens* [11,27,30,31], *Burkholderia cepacia* [16,32,33], *Candida antarctica* type B (Novozym[®] 435) [10,15,17,30,34,35], *P. cepacia* [36-40], *C. rugosa* [37], *Pseudomonas sp.* [7,26,41], *P. aeruginosa*. [42] and *Thermomyces lanuginosus* [17].

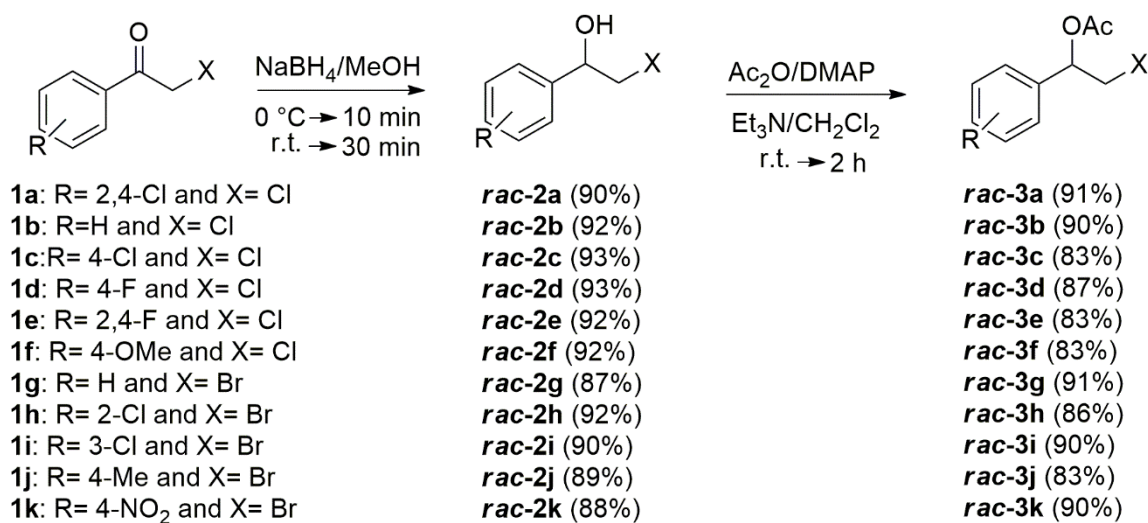
Recently, our research group reported the chemoenzymatic synthesis of the potent antifungal luliconazole [17]. The key step in the preparation of this drug was to obtain the enantiomerically pure halohydrin (1*S*)-2-chloro-1-(2,4-dichlorophenyl)-1-ethanol **2a** (Scheme 1). The latter was obtained by the kinetic resolution of the corresponding racemic acetate *rac*-**3a** (Scheme 1) via a hydrolysis reaction catalyzed by lipase from *Thermomyces lanuginosus* or Novozym[®] 435. This latter enzyme proved to be a robust biocatalyst in the kinetic resolution, leading to the (*S*)- β -halohydrin with high selectivity (*e.e.* > 99%, *E* > 200) in just 15 min, at 45 °C, and being reused for five-times with maintenance high values of both conversion and enantioselectivity. This promising result prompted us to evaluate the kinetic resolution of a series of phenylethyl halohydrins acetates *rac*-**3a-k** (Scheme 1) containing several groups attached to the aromatic ring, via the hydrolysis reaction, catalyzed by Novozym[®] 435.

Results and discussion

Syntheses of racemic halohydrins (*rac*-**2a-k**) and its acetates (*rac*-**3a-k**)

As first step, the chemical reduction of α -haloketones **1a-k** were carried out by using sodium borohydride (0.5 eq.) in MeOH [17] to yield *rac*-**2a-k** in yields ranging from 87 to 93% (Scheme 1). Next, the chemical acetylation of *rac*-**2a-k** were performed using Ac₂O, DMAP and Et₃N at room temperature for 2 h [17] and allowed the preparation of *rac*-**3a-k** in yields ranging from 83 to 91% (Scheme 1). Adequate chiral GC analyses were developed for both *rac*-**2a-k** and *rac*-**3a-k** in order to

achieve a reliable method to measure the enantiomeric excesses of both remaining substrates and the final products from the lipase-catalyzed resolution.



Scheme1. Syntheses of phenylethyl halohydrins acetates **3a-k**.

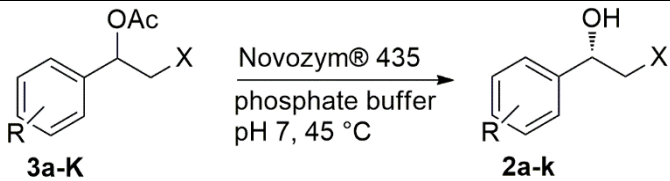
Lipase kinetic resolution of acetates *rac-3a-k* via hydrolysis catalyzed by Novozym[®] 435

The enantioselective hydrolysis of racemic 2-chloro-1-(2,4-dichlorophenyl)ethyl acetate **3a** (Scheme 1) into the corresponding (*S*)- β -halohydrin **2a** has been previously accomplished using Novozym[®] 435 (immobilized lipase B from *Candida antarctica*, CaLB), after a screening of twelve commercially available lipases [17]. After optimization of the reaction conditions, the biotransformation was carried out in phosphate buffer pH 7.0 (0.1 M), at 45°C, ratio lipase/substrate 0.5, furnishing (*S*)-2-chloro-1-(2,4-dichlorophenyl)ethanol with enantiomeric excess > 99% in correspondence of 50 % conversion ($E > 200$), after only 15 minutes [17]. Due to the hydrophobicity of the substrate **3a** ($\log P = 3.58$), the reaction was carried out in a multiphase system, with the insoluble ester forming a distinct phase. One possible explanation of the high reactivity of Novozym[®] 435 towards **3a** in a fully aqueous medium without any co-solvent, might reside in the hydrophobicity of the carrier of this lipase, which is a form of CaLB immobilized onto a microporous (poly(methylmethacrylate) resin. Consequentially, **3a** preferentially partitions onto the immobilized system suspended in water, highly facilitating the interactions between enzyme and substrate.

We further investigated the relationship between hydrophobicity of the substrates and rates of hydrolysis by experimentally performing the hydrolysis of various 2-chloro-1-phenylethyl acetates and 2-bromo-1-phenylethyl acetates derivatives with different substituents on the aromatic ring.

Firstly, the 2-chloro derivatives were enzymatically hydrolyzed using Novozym[®] 435 (Table 1, entries 1-6). The investigation about enantioselective hydrolysis of β -chlorohydrins acetates using immobilized CaLB was then extended to 2-bromo-1-phenylethyl acetates derivatives (Table 1, entries 7-11).

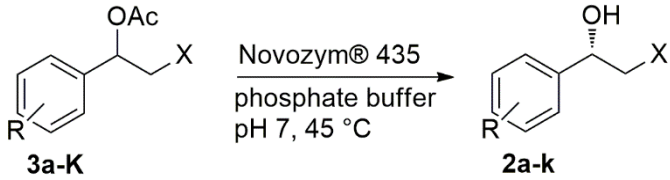
Table 1. Hydrolysis of 2-halo-1-phenylethyl acetates derivatives with immobilized CaLB.

						
Entry	Substrate	R	X	Conversion (%)	ee _p (%)	Time (h)
1	3a	2,4-Cl	Cl	50	> 99	0.25
2	3b	H	Cl	48	> 99	6
3	3c	4-Cl	Cl	50	> 99	4
4	3d	4-F	Cl	49	> 99	6
5	3e	2,4-F	Cl	48	> 99	6
6	3f	4-OMe	Cl	50	> 99	18
7	3g	H	Br	49	> 99	16
8	3h	2-Cl	Br	50	> 99	216
9	3i	3-Cl	Br	50	> 99	22
10	3j	4-Me	Br	50	> 99	20
11	3k	4-NO ₂	Br	50	> 99	192

Notably, all the biotransformations occurred with complete enantioselectivity, with formation of the (*S*)-halohydrin with ee > 99%. The time needed to reach 50% conversion (ideal for the kinetic resolution) ranged from 15 min for the 2,4-dichlorophenyl derivative **3a** (entry 1) up to 18 h observed in the case of the 4-methoxyphenyl derivative **3f** (entry 6). Enzymatic hydrolysis of derivatives **3g-k** gave the desired kinetic resolution only after days in the case of 2'-chlorophenyl derivative **3h** (entry 8) and 4-nitrophenyl derivative **3k** (entry 11).

Although an actual kinetic study of the reactions was not possible due to the complex, multiphase system employed, initial reaction rates are reported in Table 2 for a better understanding of the experimental results.

Table 2. Initial rates observed in the hydrolysis of 2-halo-1-phenylethyl acetates derivatives with immobilized CaLB.

					
Entry	Substrate	R	X	Log P	Initial rate ($\mu\text{mol}/\text{min g}_{\text{cat}}$)
1	3a	2,4-Cl	Cl	3.58	11.33
2	3b	H	Cl	2.37	2.01
3	3c	4-Cl	Cl	2.98	3.98
4	3d	4-F	Cl	2.51	1.64
5	3e	2,4-F	Cl	2.66	6.88
6	3f	4-OMe	Cl	2.21	1.20
7	3g	H	Br	2.56	0.67
8	3h	2-Cl	Br	3.16	0.20
9	3i	3-Cl	Br	3.16	0.53
10	3j	4-Me	Br	3.07	1.60
11	3k	4-NO ₂	Br	2.50	0.23

The reaction of β -chloro derivatives was generally much faster than what observed with β -bromo analogues; a comparison between the enzymatic hydrolysis of 2-chloro-1-phenylethyl acetate (**3b**, entry 2) and 2-bromo-1-phenylethyl acetate (**3g**, entry 7) indicates that the latter occurred much slower, most likely due to the higher hindrance of the bromine in 2-position.

In the case of β -brominated substrates steric hindrance on the aromatic ring plays a crucial role, as noticed by the different reaction rates for 2-chlorophenyl and 3-chlorophenyl derivatives (**3h** and **3i**, respectively), where the *meta* derivative showed higher reaction rate compared to *ortho* one. Conversely, in the case of β -chlorinated halohydrins acetates, steric effects caused by the substituted aromatic ring show no influence on the reaction, as indicated by the highest reactivity of 2,4-dichlorophenyl derivative **3a**.

It is noteworthy that the most hydrophobic substrate in the dataset (the β -chlorinated halohydrin acetate di-Cl-substituted on the aromatic ring in *ortho* and *meta* positions) expressed a reaction rate far higher in respect of the other substrates.

Computational study of (S)-halohydrin 3a-k

To clarify some details of the different reaction rates observed in the experiments docking studies of all the provided substrates have been carried out. The idea was to identify whether near attack conformation (or NAC) were observed. NACs are defined as conformations compatible with the attack of the catalytic serine to the electrophilic carbon of the acyl group [55]. In a typical NAC (such as that of Figure 1) the distance between the oxygen of Ser105 and the molecule carbonyl carbon is generally observed to be close to 3 Å, and the same atoms, together with the molecule carbonyl oxygen, generally form an angle of about 60°.

For a given target/substrate system it can be assumed that the observation of a numerous NAC population in a set of generated docking poses could imply a higher reaction rate with respect to a system in which NAC poses are not observed. Obviously, it must be also considered that in this kind of computational investigation the substrate is “forced” into the active site and the influence on the reaction rate caused by physical aspects like solubility, active site accessibility, and mass transfer are not taken into account. Nevertheless, even if crude, a docking poses assessment can give some interesting insight on the possible underlying processes.

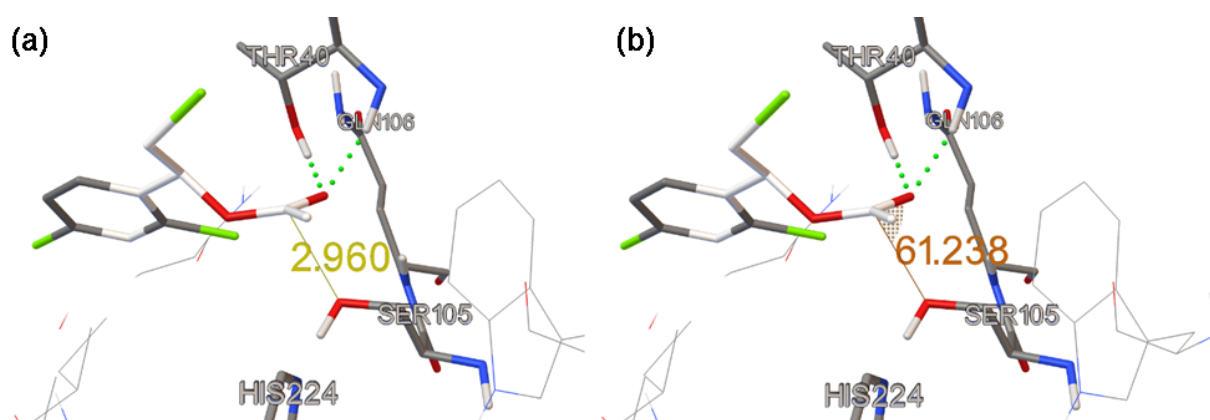


Figure 1. A typical NAC (Near Attack Conformation) of **3a** (entry 1 of Table 2), where (a) the distance between Ser-O and carbonyl-C is below 3.2 Å and (b) the Ser-O/carbonyl-C/carbonyl-O angle is below 90°. Green dotted lines indicate hydrogen bonds with the oxyanion hole. Color code: carbon (gray), oxygen (red), nitrogen (blue), chlorine (green).

For discriminating whether a pose was a NAC or not two cut-off parameters were employed [L. Corici, L. Gardossi. Understanding Potentials and Restrictions of Solvent-Free Enzymatic Polycondensation of Itaconic Acid: An Experimental and Computational Analysis]: the maximum angle formed by Ser-O/carbonyl-C/carbonyl-O set equal to 90° and the maximum distance between Ser-O and Carbonyl-C set to 3.2 Å. The oxyanionic site stabilization was also considered as a key NAC ingredient.

The docking was performed on a representative conformation of CaLB, obtained by clustering a short molecular dynamics (MD) trajectory run at 45°C and pH 7.0 by starting from the crystallographic structure 1TCA [43, 44]. The halo-phenylethyl acetate structures were generated by taking into account the clear CaLB stereoselectivity observed in the experimental data, thus only the *S* enantiomers were studied. For each provided substrate docking calculations produced 100 poses. Each pose was manually inspected: in all docking poses the angle was always comprised in the correct cut-off range and adequate oxyanion stabilization was always provided. However, the distances between Ser-O and Carbonyl-C covered a range both above and below the cut-off distance.

Docking poses were thus classified in *strong NACs* when the Ser-O and Carbonyl-C distance was below 3.0Å, *NACs* when the distance was between 3.0Å and 3.2Å, and *weak NACs* when the distance was above 3.2Å (Figure 2). Under this classification only (Br)4-NO₂ was never observed to be in the vicinity of Ser105. In the specific case of (Br)4-NO₂ the whole set of docked conformations was clearly not productive due to the hydrogen bonding of the nitro group with the oxyanion hole (Figure 3), suggesting the detrimental effect of the nitro group for the progression of the hydrolysis reaction. All the other compounds had at least one strong NAC pose, with (Cl)4-OMe presenting 10 strong NAC poses, and at least three NAC poses with Cl4-Cl observed in more than 70 strong NAC and NAC poses. The latter compound was also found in further 9 weak NAS poses. In particular if weak NACs are taken into account other 4 compounds are found to have more than 60 productive poses (Br)H, (Br)3-Cl, (Br)4-Me, and (Cl)H. Overall the fraction of productive poses for X-brominated substrates well corroborated the available experimental data, while this was not true for the X-chlorinated ones.

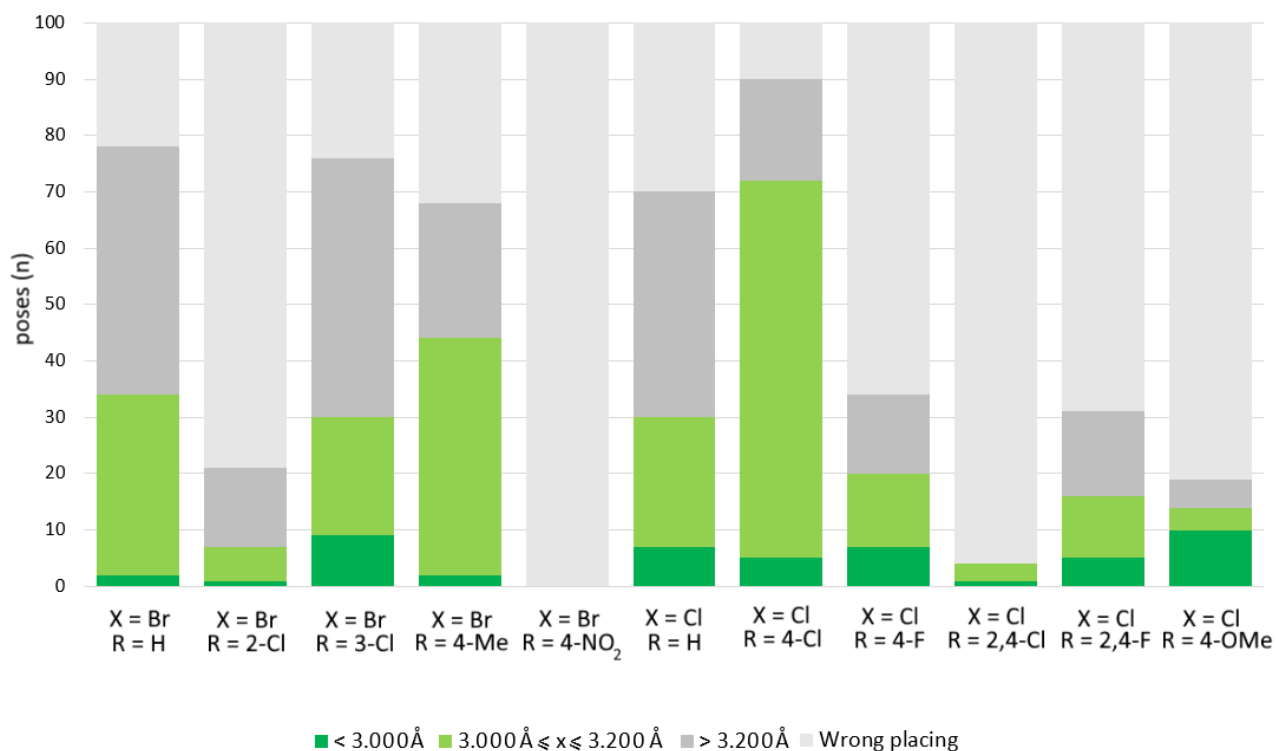


Figure 2. Graphical representation of the docked poses. Docking poses are classified as strong NACs (dark green), NACs (light green), and weak NACs (dark gray). From left to right: **3g**; **3h**; **3i**; **3j**; **3k**; **3b**; **3c**; **3a**; **3e**; **3f**.

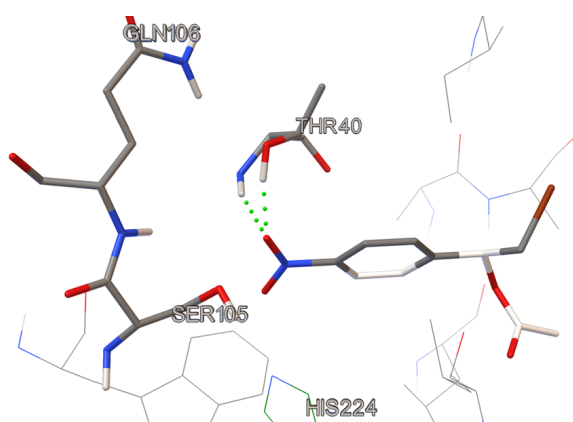


Figure 3. The most representative docked conformation of the *p*-nitro bromohydrin derivative **3k** (entry 11 of Table 2). Green dotted lines indicate hydrogen bonds with the oxyanion hole. Color code: carbon (gray), oxygen (red), nitrogen (blue), chlorine (green).

In the X-chlorinated substrates while steric features due to the presence of an *ortho*-substituent did not affect the reaction, the electronic effects of the substituents showed a non-regular effect and the docking results were different from what expected. The most fast reacting substrate 2,4-Cl presents in fact only 4 out of 100 productive poses suggesting the reasons of the high reaction rate to be related to physical aspects such as its high hydrophobicity or to a conformational change of the active site induced by this particular molecule. The most populated conformation of 2,4-Cl is found with its

carbonyl group pointing upwards, thus leading to unproductive poses according to the proposed classification (Figure 4a). On the other hand, in its lowest energy NAC pose the group is productively oriented and the distance between Ser-O and Carbonyl-C is 2.96Å (Figure 4b).

In comparison the less hydrophobic 4-fluorophenyl derivative had a larger number of productive poses than the more hydrophobic 2,4-difluorophenyl derivative, thus balancing positive docking for 4-fluorophenyl derivative and higher hydrophobicity of 2,4-difluorophenyl derivative.

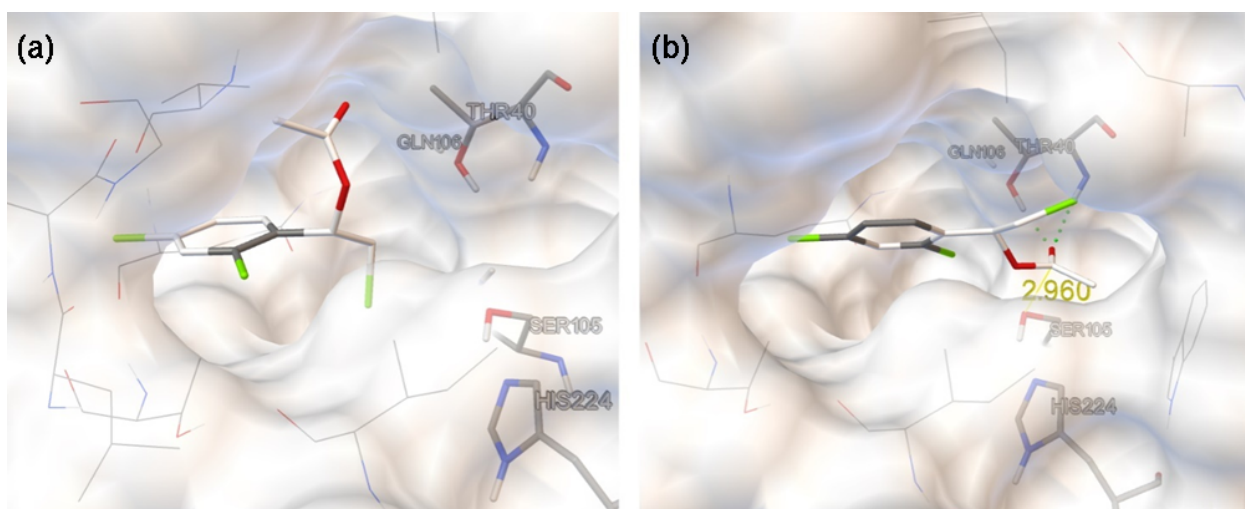


Figure 4. Docking poses of entry 1 in Table 2: (a) the most common conformation in the docking experiment (100 poses). The substrate is docked in the active site but the pose is not productive because of the unfavourable position of the ester moiety; (b) in the case of the lowest energy NAC (best electrostatic interaction between substrate and enzyme) the positioning of the substrate is optimal for the acylation to occur. Green dotted lines indicate hydrogen bonds with the oxyanion hole, the distance between Ser-O and Carbonyl-C is indicated angstrom. Color code: carbon (gray), oxygen (red), nitrogen (blue), chlorine (green).

Conclusion

In summary, commercial lipase Novozym[®] 435 was extremely efficient at kinetic resolution (KR) of eleven phenylethyl halohydrins acetates, leading to the corresponding (*S*)- β -halohydrins with ee > 99% ($E > 200$) and 50% conversion. The volume of the halogen atom played a crucial role in the KR, with the reaction of β -chloro derivatives being much faster than what observed with β -bromo analogues. The position and size of the substituents attached to the aromatic ring only influenced the β -bromo acetates and did not influence the KR rate of the β -chloro derivatives. Docking studies using MD simulations revealed that bromohydrins acetates produced a smaller number of productive poses

relative to the chlorohydrins derivatives, corroborating with the experimental fact that these first ones are less reactive in the KR catalyzed by Novozym[®] 435. Interestingly, steric features due to the presence of an *ortho*-substituent or electronic effects of the substituents did not show a regular effect for the chlorohydrins acetates. In this case, the results obtained in the computational studies differ from expectations. In general, the amount of productive poses for chlorohydrins acetate was not so high to justify its greater reactivity. These results suggest that the high reactivity of β -chlorohydrins acetates is more closely related to physical aspects such as hydrophobicity or induced change in the conformation of the enzymatic active site than to electronic or steric hindrance.

Experimental

Computational

The crystal structure of CaLB 1TCA [43, 44] was taken from the Protein Data Bank [43] and was pre-processed with PyMOL (The PyMOL Molecular Graphics System, Version 1.5.0.4 Schrödinger, LLC) by removing all water molecules and ligands. The protonation state was computed at pH 7.0 using the PROPKA-based [45] PDB2PQR online server [46]. The structure was inserted in a 343 nm³ water box, while including sodium and chloride ions at the concentration of 0.1 M in the correct proportion to neutralize the charge of the system. OPLS-AA force-field [47] and TIP4 water model [49] were employed. A minimization was performed with 10000 steepest descent steps. The system was then equilibrated for 5ns followed by 5ns of production molecular dynamics run at 45° C in NVT ensemble using Particle Mesh Ewald (PME) algorithm [50] for the calculation of electrostatic interactions, and keeping the temperature and pressure constant (ν -rescale algorithm [51] for temperature and Berendsen algorithm [52] for pressure). The structure to be used for the docking was identified by using the *g_cluster* tool to extract the most representative conformation in the production trajectory file as implemented in the GROMACS package version 4 [48].

The halo-phenylethyl acetate structures were generated as *S* enantiomers with PyMOL. Their geometries were optimized in Avogadro version 1.2. All the structures were processed using a Lamarckian genetic algorithm that was run 100 times, each one comprising 250 docking poses. Eventually the best 100 poses were selected according to AutoDock scoring function based on

binding energy. AutoDock version 4.2 was used for docking [53, 54]. A visual inspection of the poses allowed to extract the Near Attack Conformation (NAC) poses corresponding to the productive ones.

Chemical Materials

C. antarctica lipase type B immobilized on acrylic resin (CAL-B, Novozym 435, 7,300.0 U/g) was purchased from Novozymes[®]. Chemical reagents were purchased from different commercial sources and used without further purification. Solvents were acquired from Synth. Solvents were distilled over an adequate desiccant under nitrogen. Analytical TLC analyses were performed on aluminum sheets pre-coated with silica gel 60 F254 (0.2 mm thick) from Merck[®]. Flash chromatographies were performed using silica gel 60 (230-240 mesh).

Analysis

Melting points were determined in open capillary tube Microquímica model MQAPF-302 and are uncorrected. ¹H and ¹³C NMR were obtained using Spectrometers Bruker model Avance DPX 300 and Avance DRX-500 MHz, operating at frequencies of 300 MHz and 500 MHz for hydrogen and frequencies of 75 MHz and 125 MHz for carbon, respectively. The chemical shifts are given in delta (δ) values and the coupling constants (J) in Hertz (Hz). Measurement of the optical rotations were done in a Jasco P-2000 polarimeter. Gas chromatograph (GC) analyses were carried out in a Shimadzu chromatograph model GC 2010 with a flame ionization detector. A table to put all results supporting information. The analysis of acetates **3a** and **3e** and halohydrins **2a** and **2e** was carried out using a chiral column CP-chirasil-dex (25 m x 0.25 mm x 0.25 μ m, 0.5 bar N₂). For the monitoring of the reaction time courses of *rac*-2-chloro-1-(2,4-dichlorophenyl)ethyl acetate (*rac*-**3a**) the following conditions were used: 185 °C; 1 °C/min. 190 °C (hold 5 min.); 0.5 °C/min. 200 °C (hold 15 min.). Retention times were: (*R*)-acetate **3a** = 8.33 min.; (*S*)-acetate **3a** = 8.82 min.

Halohydrin *rac*-**2a** was analyzed using a chiral column Rt-BDEXcst (30 m x 0.39 mm x 0.25 μ m, 0.5 bar N₂) and the reaction time courses were monitored using the following conditions: 185 °C; 1 °C/min. 190 °C (hold 5 min.); 0.5 °C/min. 200 °C (hold 15 min.). Retention times were: (*S*)-halohydrin **2a** = 17.90 min.; (*R*)-halohydrin **2a** = 18.50 min.

General procedure for syntheses of *rac*- β -halohydrins (*rac*-**2a-k**)

NaBH₄ (0.085 g, 2.2 mmol) was slowly added to a solution of α -chloroketones **1a-k** (4.5 mmol) in MeOH (40 mL) at 0 °C. The reaction was stirred for 30 min at room temperature. Upon completion, the MeOH was evaporated under reduced pressure. Then, 1 M HCl (10 mL) was added followed by extraction with EtOAc (4 x 60 mL). Organic phases were combined and dried over anhydrous

Na₂SO₄, filtered and solvent was evaporated under reduced pressure. Then, the crude product was purified by performing column chromatography, employing silica gel and CHCl₃ to afford *rac*-β-halohydrins *rac-a-k* in yields ranging from 87 to 93%.

General procedure for syntheses of synthesis of *rac*-acetates (*rac-3a-k*)

A suspension of DMAP (0.054 g, 0.4 mmol) and acetic anhydride (1.25 mL, 13.3 mmol) was dissolved in CH₂Cl₂ (40 mL). Then, *rac-2a-k* (4.4 mmol) and triethylamine (616.3 μL, 4.4 mmol) were added. The reaction was stirred for 2 h at room temperature. After this time, distilled water (10 mL) was added followed by extraction with CH₂Cl₂ (3 x 50 mL). The organic phases were combined and dried over anhydrous Na₂SO₄. Then, after filtration, the solvent was evaporated under reduced pressure and the crude product was purified using a silica gel column chromatography and CHCl₃ to afford *rac*-acetates *rac-3a-k* in yields ranging from 83 to 91%.

General procedure for the enzymatic kinetic resolution of *rac*-acetates (*rac-3a-k*) catalyzed by Novozym[®] 435

A suspension of *rac*-acetate (*rac-3a-k*) (0.1 mmol) and lipase (ratio 0.5:1 in weight respect to the *rac-3*) in phosphate buffer 100 mM pH 7.0 (1.0 mL) was shaken at 45°C and in their proper time reaction at 250 rpm. After the conversion reaches a value close to 50%, the products were extracted with EtOAc (3 x 5 mL). The organic phases were combined and dried over Na₂SO₄, filtered and the solvent evaporated under reduced pressure. The reaction crude was purified by flash chromatography on silica gel (100% CHCl₃), yielding (*R*)-acetates (*R-3a-k*) and (*S*)-halohydrins (*S-2a-k*) being their enantiomeric excess determined by GC.

Physical data (melting point and optical rotation) and spectroscopic data (NMR)

Acknowledgements

The authors thank to the Fundação Cearense de Apoio ao Desenvolvimento Científico e Tecnológico (FUNCAP), Conselho Nacional de Desenvolvimento Científico e Tecnológico (CNPq) and Coordenação de Aperfeiçoamento de Ensino Superior (CAPES) for fellowships and financial support. The authors thank the Brazilian funding agency Conselho Nacional de Desenvolvimento Científico e Tecnológico (CNPq) for providing the Special Visiting Researcher fellowship (process 400171/2014-7) under the Brazilian Scientific Program “Ciência sem Fronteira” and the research

sponsorships of M. C. de Mattos (Process: 308034/2015-5) and M. C. F. de Oliveira (Process: 303365/2014-5). The authors thank the Northeastern Center for Application and Use of NMR (CENAUREMN) for NMR spectroscopy. L.G. acknowledges Università degli Studi di Trieste (FRA 2018) for financial support.

References

- [1]. J. S. Yadav, B. V. S. Reddy, C. S. Reddy, K. Rajasekhar, *Chem. Lett.* 33 (2004) 476-477.
- [2]. K. Surendra, N. Krishnaveni, V. P. Kumar, Y. V. D. Nageswar, K. R. Rao, *Lett. Org. Chem.* 2 (2005) 652-658.
- [3]. R. M. A. Pinto, J. A. R. Salvador, C. L. Roux, *Tetrahedron* 63 (2007) 9221-9228.
- [4]. J. Zhang, J. Wang, Z. Qiu, Y. Wang, *Tetrahedron* 67 (2011) 6859-6867.
- [5]. M. A. K. Zarchi, A. Tarabsaz, *J. Polym. Res.* 208 (2013) 1-9.
- [6]. B. Tamami, H. Mahdavi, *React. Funct. Polym.* 51 (2002) 7-13.
- [7]. U. Ader, M. P. Schneider, *Tetrahedron: Asymmetry* 3 (1992) 521-524.
- [8]. C. Lu, Z. Luo, L. Huang, X. Li, *Tetrahedron: Asymmetry* 22 (2011) 722-727.
- [9]. B. P. Dwivedee, S. Ghosh, J. Bhaumik, L. Banoth, U. C. Banerjee, *RSC Adv.* 5 (2015) 15850-15860.
- [10]. I. T. Lund, P. L. Bøckmann, E. E. Jacobsen, *Tetrahedron* 72 (2016) 7288-7292.
- [11]. G. V. Lima, M. R. da Silva, T. S. Fonseca, L. B. de Lima, M. C. F. de Oliveira, T. L. de Lemos, D. Zampiere, J. C. S. dos Santos, N. S. Rios, L. R. B. Gonçalves, F. Molinari, M. C. de Mattos, *Appl. Catal. A* 546 (2017) 7-14.
- [12]. E. J. Corey, G. A. Reichard, *Tetrahedron Lett.* 30 (1989) 5207-5210.
- [13]. D. W. Robertson, J. H. Krushinski, R. W. Fuller, J. D. Leander, *J. Med. Chem.* 31 (1988) 1412-1417.
- [14]. J.-N. Zhou, Q. Fang, Y.-H. Hu, Li.Y. Yang, F.-F. Wu, L.-J. Xie, J. Wu, S. Li, *Org. Biomol. Chem.* 12, (2014) 1009-1017.
- [15]. H. Liu, B. H. Hoff, T. Anthonsen, *Chirality* 12 (2000) 26-29.
- [16] J. M. Sánchez, E. Busto, Vicente G.-Fernández, F. Malpartida, V. Gotor, *J. Org. Chem.* 76 (2011) 2115-2122.
- [17]. T. S. Fonseca, L. D. Lima, M. C. F. de Oliveira, T. L. G. de Lemos, D. Zampieri, F. Molinari, M. C. de Mattos, *Eur. J. Org. Chem.* (2018) 2110-2116.

- [18] P. B. Thorat, S. V. Goswami, V. P. Sondankar, S. R. Bhusare, *Chi. J. Catal.* 36 (2015) 1093-1100.
- [19]. E. J. Corey, C. J. Helal, *Angew. Chem. Int. Ed.* 37 (1998) 1986-2012.
- [20]. T. Ohkuma, K. Tsutsumi, N. Utsumi, N. Arai, R. Noyori, K. Murata, *Org. Lett.* 9 (2007) 255-257.
- [21]. A. Ros, A. Magriz, H. Dietrich, R. Fernández, E. Alvarez, J. M. Lassaletta, *Org. Lett.* 8 (2006) 127-130.
- [22]. F. Martinez-Lagos, J. V. Sinisterra, *J. Mol. Catal. B: Enzym.* 36 (2005) 1-7.
- [23]. H. Lin, Y.-Z. Chen, X.-Y. Xu, S.-W. Xia, L.-X. Wang, *J. Mol. Catal. B: Enzym.* 57 (2009) 1-5.
- [24]. G.-C. Xu, H.-L. Yu, Y.-P. Shang, J.-H. Xu, *RSC Adv.* 5 (2015) 22703-22711.
- [25]. M. L. Contente, I. Serra, F. Molinari, R. Gandolfi, A. Pinto, D. Romano, *Tetrahedron* 72 (2016) 3974-3979.
- [26]. W. Adam, L. Blancafort, C. R. saha-Möller, *Tetrahedron: Asymmetry* 8 (1997) 3189-3192.
- [27]. I. M. Ferreira, S. A. Yoshioka, J. V. Comasseto, A. L. M. Porto, *RSC Adv.* 7 (2017) 12650-12658.
- [28]. V. Gotor-Fernández, R. Brieva, V. Gotor, *J. Mol. Catal. B: Enzym.* 40 (2006) 111-120.
- [29]. A. C. L. M. Carvalho, T. S. Fonseca, M. C. de Mattos, M. C. F. de Oliveira, T. L. G. de Lemos, F. Molinari, D. Romano, I. Serra, *Int. J. Mol. Sci.* 16 (2015) 29682-29716.
- [30]. S. Conde, M. Fierros, M. I. Rodríguez-Franco, C. Puig, *Tetrahedron: Asymmetry* 9 (1998) 2229-2232.
- [31]. J. Hiratake, M. Inagaki, T. Nishioka, J. I. Oda, *J. Org. Chem.* 53 (1988) 6130-6133.
- [32]. L. H. Andrade, L. P. Rebelo, C. G. C. M. Netto, H. E. Toma, *J. Mol. Catal. B: Enzym.* 66 (2010) 55-62.
- [33]. T. Itoh, Y. Matsushita, Y. Abe, S.-h. Han, S. Wada, S. Hayase, M. Kawatsura, S. Takai, M. Morimoto, Y. Hirose, *Chem. Eur. J.* 12 (2006) 9228-9237.
- [34]. A. Träff, K. Bogár, M. Warner, J.-E. Bäckvall, *Org. Lett.* 10 (2008) 4807-4810.
- [35]. M. Kapoor, N. Anand, K. Ahmad, S. Koul, S. S. Chimi, S. C. Taneja, G. N. Qazi, *Tetrahedron: Asymmetry* 16 (2005) 717-725.
- [36]. A. Kamal, M. Sandbhor, K. V. Ramana, *Tetrahedron: Asymmetry* 13 (2002) 815-820.
- [37]. K.-W. Kim, B. Song, M.-Y. Chol, M.-J. Kim, *Org. Lett.* 3 (2001) 1507-1509.
- [38]. F. Campos, M. P. Bosch, A. Guerrero, *Tetrahedron: Asymmetry* 11 (2000) 2705-2717.
- [39]. S. M. Lystvet, B. H. Hoff, T. Anthonsen, E. E. Jacobsen, *Biocatal. Biotransform.* 28 (2010) 272-278.
- [40]. E. Fuglseth, T. Anthonsen, B. H. Hoff, *Tetrahedron: Asymmetry* 17 (2006) 1290-1295.

- [41]. O. Pàmies, J.-E. Bäckvall, *J. Org. Chem.* 67 (2002) 9006-9010.
- [42]. T. Ema, N. Ura, M. Yoshii, T. Korenaga, T. Sakai, *Tetrahedron* 65 (2009) 9583-9591.
- [43] H. M. Berman, J. Westbrook, Z. Feng, G. Gilliland, T. N. Bhat, H. Weissig, I. N. Shindyalov, P. E. Bourne, *Nucleic Acids Res.* 28 (2000) 235–242.
- [44] J. Uppenberg, M. T. Hansen, S. Patkar, T. A. Jones, *Structure* 2 (1994) 293–308.
- [45] C. R. Sondergaard, M. H. M. Olsson, M. Rostkowski, J. H. Jensen, *J. Chem. Theory Comput.* 7 (2011) 2284-2295.
- [46] T. J. Dolinsky, J. E. Nielsen, J. A. McCammon, N. A. Baker, *Nucleic Acids Res.* 32 (2004) W665-W667.
- [47] G. A. Kaminski, R. A. Friesner, J. Tirado-Rives, W. L. Jorgensen, *J. Phys. Chem. B* 105 (2001) 6474-6487.
- [48] B. Hess, C. Kutzner, D. van der Spoel, E. Lindahl, *J. Chem. Theory Comput.* 4 (2008) 435-447.
- [49] H. W. Horn, W. C. Swope, J. W. Pitera, J. D. Madura, T. J. Dick, G. L. Hura, T. Head-Gordon, *J. Chem. Phys.* 120 (2004) 9665-9678.
- [50] U. Essmann, L. Perera, M. L. Berkowitz, T. Darden, H. Lee, L. G. Pedersen, *J. Chem. Phys.* 103 (1995) 8577-8592.
- [51] G. Bussi, D. Donadio, M. Parrinello, *J. Chem. Phys.* 126 (2007) 126 014101.
- [52] H. J. C. Berendsen, J. P. M. Postma, W. F. van Gunsteren, A. Di Nola, J. R. Haak, *J. Chem. Phys.* 81 (1984) 3684-3690.
- [53] G. M. Morris, R. Huey, W. Lindstrom, M. F. Sanner, R. K. Belew, D. S. Goodsell, A. J. Olson, *J. Comput. Chem.* 30 (2009) 2785–2791.
- [54] G. M. Morris, D. S. Goodsell, O. S. Halliday, R. Huey, W. E. Hart, R. K. Belew, A. J. Olson, *J. Comput. Chem.* 19 (1998) 1639–1662.
- [55] T. C. Bruice, F. C. Lightstone, *Acc. Chem. Res.* 32 (1999) 32 127–136.